

Two-Photon Excitation Spectrum of Light-Harvesting Complex II and Fluorescence Upconversion after One- and Two-Photon Excitation of the Carotenoids

Peter J. Walla, Jenny Yom, Brent P. Krueger, and Graham R. Fleming*

Department of Chemistry, University of California at Berkeley, and Physical Biosciences Division, Lawrence Berkeley National Laboratory, Berkeley, California 94720

Received: December 7, 1999; In Final Form: February 22, 2000

The two-photon excitation (TPE) spectrum of light-harvesting complex II (LHC II) has been measured in the spectral region of 1000–1600 nm, corresponding to one-photon wavelengths of 500–800 nm. We observed a band with an origin at $\sim 2 \times 660$ nm (ca. $15\,100 \pm 300$ cm⁻¹) and a maximum at $\sim 2 \times 600$ nm. The line shape and origin of this band strongly suggest that the observed signal is due to the two-photon-allowed S₁ state of the energy-transferring carotenoids (Car) in LHC II. We also report the time dependence of the upconverted chlorophyll (Chl) fluorescence after TPE at the maximum of the observed band. Surprisingly, a fast rise of 250 ± 50 fs followed by a multiexponential decay on the picosecond time scale was observed. This result provides strong indication that there is a fast energy transfer even from the dipole-forbidden Car S₁ state to the Chl's. The sub picosecond energy transfer from the Car S₁ state is likely a consequence of the large number of energy-accepting Chls in van der Waals contact with the central Car's in LHC II. We also present upconversion data of the Car S₂, Chl *a*, and Chl *b* fluorescence observed after one-photon excitation into the dipole-allowed Car S₂ state. The lifetime of the Car S₂ state is $\sim 120 \pm 30$ fs. With the observed time constants we are able to calculate quantum yields for the different possible pathways contributing to the overall Car to Chl energy transfer in LHC II.

Introduction

The most abundant light-harvesting protein of green plants is light-harvesting complex II (LHC II).^{1–3} Over half the light used for photosynthesis is collected by the chromophores in this protein. In the thylakoid membranes of chloroplasts they serve as the primary donors of the electronic excitation energy, which is funneled to the reaction centers and finally converted into chemically storable energy.

Each LHC II monomer contains 7–8 chlorophyll *a* (Chl *a*), 5–6 chlorophyll *b* (Chl *b*), and roughly 3–3.5 carotenoid (Car) molecules. The Car's of one LHC II monomer are roughly two luteins, one neoxanthin, and a substoichiometric amount of violaxanthin.^{3–5} In the 3.4 Å crystal structure of the LHC II from Kühlbrandt and co-workers, only two Car's are fully resolved.⁶ They have an almost C₂-symmetrical position in the center of the resolved structure and are surrounded by at least seven Chl's in van der Waals contact and five Chl's in close proximity. Recent work of Bassi and co-workers showed that these two Car sites have the highest affinity to lutein.⁷ One of the central Car sites also can be occupied by a violaxanthin. The other resolved site shows affinity only to lutein, whereas an unresolved third site has affinity to neoxanthin.

The main function of the Chls is light-harvesting in the blue (Soret transitions) and the red (Q_y and Q_x transitions) regions of visible light (Figure 1). In contrast, the function of the carotenoids is at least 3-fold: they also serve as light-harvesting molecules in the blue-green region, they quench Chl triplet states to prevent the creation of dangerous singlet oxygen, and they play an important structural role. It was also proposed that they serve an important function by regulating the flow of excessive excitation energy from the antenna to PSII reaction center via the xanthophyll cycle.^{8–10} However, this function may be

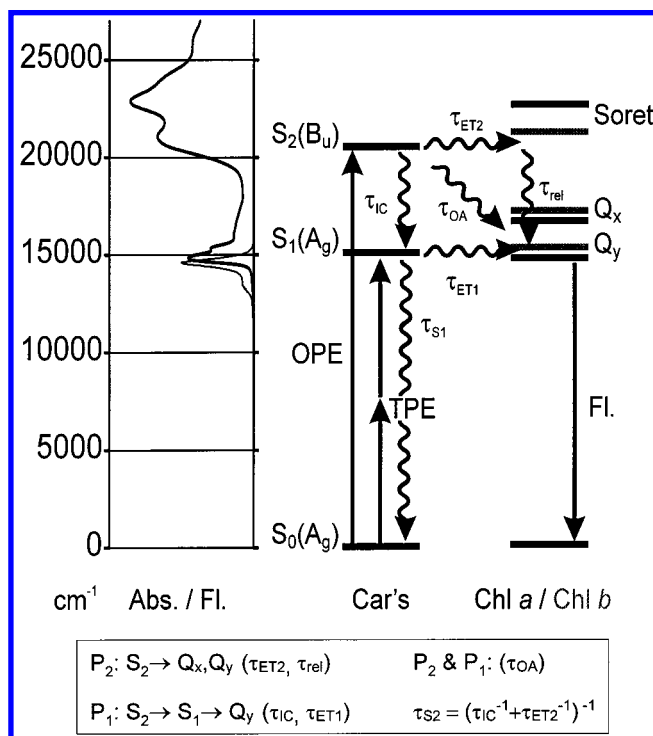


Figure 1. Left: Absorption (thick line) and fluorescence (thin line) of LHC II. Right: Energetic diagram for LHC II. OPE: one-photon excitation. TPE: two-photon excitation. FI: Fluorescence. For definitions of the time constants see the text.

associated more with the carotenoids in the minor antennas such as CP 26 and CP 29.¹¹ The aim of this work is to investigate the first-mentioned function, the mechanism of the light-harvesting of the carotenoids in LHC II.

It is known that the energy transfer (ET) of singlet excitation from Car's to Chl is very efficient ($\sim 80\%$).^{12,4} In two different reports of transient absorption experiments with LHC II the characteristic time constant for the overall Car–Chl ET, τ_{OA} , measured as the rise in excited Chl population was found to be ultrafast. Peterman et al. found ET predominantly to Chl *a* with a time constant, τ_{OA} , of 220 ± 25 fs at 77 K. Connelly et al. found ET predominantly to Chl *b* with a value for τ_{OA} of 142 fs at room temperature.^{12,13} The Car's possess two states corresponding to transitions in the region of visible light: S_2 , which is located just below the Chl *b* Soret transition at $\sim 20\,000$ cm^{-1} , and S_1 , which has an energy similar to that of the Chl Q_y transitions ($\sim 15\,000$ cm^{-1}) (Figure 1). However, only the transition to S_2 has a significant transition dipole moment, and therefore only S_2 can contribute to the primary light-harvesting of Car's. To understand this, the electronic states of carotenoids are often described in analogy to polyenes: Their ground state (S_0) and first excited state (S_1) both possess A_g symmetry; their second excited state (S_2) possesses B_u symmetry in the idealized C_{2h} point group. Carotenoids do not adhere strictly to C_{2h} symmetry but still possess many of the spectral characteristics of the parent polyenes from which they were derived. Therefore, according to the selection rules for optical transitions, only the $S_0 \leftrightarrow S_2$ transition is optically dipole-allowed and contributes significantly to the absorption spectrum of Car's. However, it is known from isolated Car's, that after excitation into S_2 they undergo rapid internal conversion (IC) to the S_1 state. This time constant, τ_{IC} , for lutein in solution is ~ 200 – 230 fs (Gillbro, unpublished results).¹² Recently, it has been shown that for the very similar carotenoid, β -carotene, τ_{IC} only varies from 120 fs (quinoline) to 177 fs (hexane) in different solvents.¹⁴ The lifetime of S_1 in solution, τ_{S_1} , is ~ 10 – 20 ps.

There has been a long debate about the mechanism of the Car–Chl ET in different light-harvesting species. Starting at the Car S_2 state, the energy can generally flow via two pathways: One pathway, P_2 , could be a fast ET directly from the Car S_2 to Chl states, $\tau_{\text{ET}2}$, with subsequent relaxation, τ_{rel} , to the Chl a Q_y state (Car $S_2 \rightarrow$ Chl Q_x , Q_y). However, for P_2 to be the main contribution to the ET the time constant $\tau_{\text{ET}2}$ must be very fast to compete against the fast IC to S_1 in the carotenoid, τ_{IC} . Since both the donating state (Car S_2) and the accepting state (Chl Q_x or Q_y) correspond to strongly dipole-allowed transitions, a standard Coulombic coupling mechanism^{15,16} could explain a rapid rate. However, to be more than 80% efficient, the time constant $\tau_{\text{ET}2}$ must be on the order of 50 fs, which seems unlikely, considering the comparable protein PCP, for which we can conclude that the pairwise ET from the Car's S_2 state is $\tau_{\text{ET}2} > 600$ fs. Note that the much faster ET ($\tau_{\text{ET}2} \approx 50$ fs) observed in bacterial systems¹⁷ has its origin in the location of the bacteriochlorophyll (BChl) Q_x state, which is much more favorable for accepting energy from the Car S_2 state. The other pathway, P_1 , could be first IC from S_2 in about 200 fs (τ_{IC}) to S_1 , and then ET from S_1 , $\tau_{\text{ET}1}$, to Q_y (Car $S_2 \rightarrow$ Car $S_1 \rightarrow$ Chl Q_y). Since the natural S_1 lifetime (τ_{S_1}) is much longer (10–20 ps) than the natural S_2 lifetime (τ_{IC}), a more reasonable ET time constant $\tau_{\text{ET}1}$ of about 1 ps would be sufficient to explain the high overall ET efficiency from Car's to Chl's. However, in a pure P_1 scenario the roughly 100–200 fs measured for τ_{OA} would require $\tau_{\text{ET}1}$ to also be ultrafast. This would be in contrast to measurements of $\tau_{\text{ET}1}$ in other light-harvesting systems, which are in the picosecond regime.^{18–20}

One reason for the slower τ_{ET} is that the donor transition is dipole-forbidden. It still remains a challenge to describe this Car S_1 to Chl ET theoretically. Neither the Coulombic coupling¹⁵

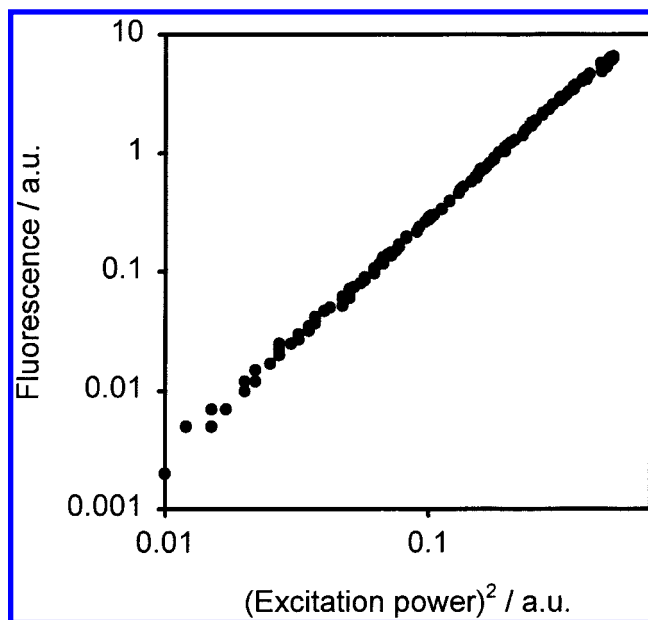


Figure 2. Dependence of the fluorescence intensity of LHC II ($\lambda_{\text{det}} \approx 685$ nm) on the two-photon excitation power at 1200 nm.

nor electron exchange²¹ mechanisms will give rapid rates. In the case of LHC II, we have also to take into account the presence of at least seven Chl's in van der Waals contact with the Car's and five others nearby. This, of course, can strongly accelerate the energy transfer for both pathways.

The only way to determine the branching between P_2 and P_1 ET is to measure the lifetime of the Car S_2 state. This can be done by measuring the time dependence of the S_2 fluorescence, since the S_2 fluorescence is not convoluted by Chl kinetics and contributions of P_1 ET as is the case in most pump–probe experiments. When the time constant for the Car S_2 to S_1 internal conversion, τ_{IC} , is known, $\tau_{\text{ET}2}$ and the quantum yield of P_2 can be calculated in a straightforward way (Figure 1).

The simplest method to determine a contribution of P_1 to the overall time constant, τ_{OA} , is to excite selectively the S_1 state of the Car's and thereby measure $\tau_{\text{ET}1}$ exclusively. Selective excitation of S_1 can be achieved by two-photon excitation (TPE), because transitions between states of symmetry A_g , such as $S_0(A_g)$ and $S_1(A_g)$, are two-photon-allowed.²² In contrast, the dipole-allowed (one-photon-allowed) transitions in Car's and Chl's are generally two-photon-forbidden. To be able to estimate possible contributions of directly excited Chl via TPE, we first have measured the TPE spectrum in the whole spectral region of the expected Car S_1 and the Chl Q states. With this spectrum it was possible to locate the 0–0 transition of the energy-transferring Car S_1 states at approximately $15\,100 \pm 300$ cm^{-1} . Measuring $\tau_{\text{ET}1}$ after TPE of S_1 can be most reliably done by upconverting the Chl fluorescence, because with this technique there is no doubt about the observed species, in contrast to transient absorption measurements.

In this paper we describe the TPE spectrum of LHC II and the upconverted Chl *a* fluorescence obtained after TPE in the maximum of the S_1 transition. We also describe the upconverted Car S_2 and Chl *a* and *b* fluorescence obtained after one-photon excitation (OPE) of the Car S_2 state at 500 (20 000 cm^{-1}) and 510 (19 600 cm^{-1}) nm. The observed kinetics are in good agreement with previous results from transient absorption experiments.^{12,13,23–25} Taking all pieces of information together, we are able to estimate the quantum yields of the different pathways contributing to the overall Car to Chl ET in LHC II.

Materials and Methods

LHC II was prepared from the PSI–PSII double-deficiency strain C2 of *Chlamydomonas reinhardtii* and purified using the methods described earlier.²⁶ According to HPLC analysis the Car composition was ~2:0.9 lutein/neoxanthin (in *C. reinhardtii* some of the lutein (~30%) is substituted by the very similar carotenoid linoxanthin) and substoichiometric amounts of violaxanthin (~0.5). The samples were stored at -70°C . To minimize scattering, each thawed LHC II sample was sonicated and centrifuged (8000 rpm, 8 min) immediately prior to the measurement. The sample was flowed through a 1 mm path length quartz cell using a peristaltic pump and maintained at $4\text{--}6^{\circ}\text{C}$ by a recirculating bath that flowed around the sample reservoir. The TPE spectrum measurement was repeated with a LHC II preparation from spinach kindly provided by the group of van Amerongen and co-workers. The preparation and purification of this sample has been described earlier.²⁷ The spectrum measured with this preparation showed no significant difference from the spectrum of the *C. reinhardtii* preparation.

Excitation light, tunable throughout the region of interest, was provided by a Coherent 9450 optical parametric amplifier (OPA). The OPA was pumped by a Coherent RegA 9000 regenerative amplifier with a model 9150 stretcher/compressor and a Mira Seed Ti:sapphire oscillator. A part (10%) of the compressor output was used as gate pulses in the upconversion experiments. The RegA 9000 was operated at a 250 kHz repetition rate that yielded pulse energies of ~10 nJ from the tunable idler beam of OPA. Typical pulse widths were ~85 fs and were fairly constant over the entire tuning range. To suppress any white light or OPA signal output, we used different dichroic mirrors (CVI 0158–791–16F, CVI 0158–791–15F) for the idler output and filtered the idler pulse with two long-wavelength pass filters (CVI LPF-110 FLN 4–8).

The TPE spectrum was measured as described earlier.²⁸ Modulated excitation light was focused into the sample with an $f = 5$ cm lens. Focusing too tightly was found to saturate rather than to increase the signal.²² Fluorescence was collected at 90° with an $f = 2.5$ cm lens, filtered with a short-wavelength pass filter (CVI SPF-950) and interference filter (Oriol P/N 5390 OJCA, 680 ± 5 nm), and recorded with a photomultiplier tube (Hamamatsu R928) connected to a lock-in amplifier (EG&G Princeton Applied Research model 5209). A portion of the excitation light was monitored parallel to the lock-in amplifier signal by a power meter (Coherent Fieldmaster GS). At each wavelength, we recorded the dependence of the fluorescence signal, F , on the excitation power, I_0 , over 2 orders of magnitude and the pulse width, δt , of the excitation pulse (Figure 2). At the highest powers we observed some saturation effects. To verify a quadratic dependence of our signal F on I_0 we fitted every power dependence curve to $F = F_0 + \sigma_1 I_0 + \sigma_2 I_0^2$, where F_0 is a constant background and σ_1 and σ_2 are relative absorption cross sections for one-photon and two-photon excitation, respectively. F_0 was found to be zero for all excitation wavelengths, and the maximum of $\sigma_1 I_0$ was at least 250 times smaller than the maximum of $\sigma_2 I_0^2$ ($\lambda_{\text{exc}} \approx 2 \times 600$ nm). σ_2 was then corrected for wavelength-dependent fluctuations of the pulse width, δt , by $\sigma_{\text{corr}} = \sigma_2 \delta t$, where σ_{corr} is the corrected cross section we finally used for Figure 3.²⁹

Fluorescence upconversion experiments have been described previously.^{17,30,31} Briefly, the same sample cell was placed in one focus of an ellipsoidal mirror and the sample was excited under the same conditions as for the TPE spectrum measurement. The spontaneous emission from the sample was collected by the ellipsoidal reflector and focused into the upconversion

crystal (0.5 mm BBO, Superoptonics no. 4824 AC–XTB-800). The residual pump beam after the sample cell was spatially blocked with a small metal rod in a position between the mirror and crystal, where the majority of the collected fluorescence was still able to pass. The constant background due to doubled light from the gate beam was reduced by a factor of 10 by cutting the blue wing of the gate beam with a 760 nm cutoff filter. The upconverted fluorescence (685 nm) was collected with a lens and focused, after spatially filtering, into the entrance slit of a double monochromator. Finally, the spectrally selected light was detected with a photomultiplier tube using gated photon counting (Stanford Research Systems SR400).

The temporal profile of the pump pulse corresponding to two-photon intensities is different from that for one-photon intensities. Therefore, for the TPE instrument response function (IRF) we used the cross correlation corresponding to two photons of the pump beam and one photon of the gate beam. This cross correlation was easily observed by tuning the monochromator and crystal angle to the wavelength of this three-photon mixing process (ca. 367 nm). We recorded the IRF in two ways. First, we flowed a clear buffer through the sample cell and removed the small rod to unblock the pump beam and measured the cross correlation. We then replaced the small rod and used a scattering solution instead of the buffer. We found no differences in time zero and only minor differences in the line shape of both cross correlation profiles. The fwhm of the instrument response function in the TPE experiments was 140 fs (Figure 4). Note that the IRF for the upconversion setup with TPE is narrower than the IRF with OPE (> 160 fs, depending on the particular experiment) because the temporal line shape of a TPE pulse is a factor of $\sqrt{2}$ narrower than the corresponding one-photon pulse width since it is the square of the one-photon pulse. Furthermore, infrared light is much less affected by dispersion than visible light.

We used three different LHC II samples and accumulated about 30 h. We monitored the amount of photodegradation over time by binning the data in 5 min increments. We also measured the absorption spectra, fluorescence spectra, and fluorescence excitation spectra before and after every measurement. The intensity of the upconversion signal was constant to within 1% during the entire period of the longest measurement (11 h). However, after the measurement this sample showed a somewhat (~6%) decreased intensity of the Chl *b* peaks at 650 and 475 nm.

Results

In Figure 3 the TPE spectrum of LHC II is plotted together with the absorption and fluorescence spectrum. It shows only small features in the spectral range of the Chl Q-bands. The onset of the TPE spectrum is at $\sim 1320 \pm 20$ nm corresponding to a one-photon wavelength of $\sim 660 \pm 10$ nm (ca. $15\,100 \pm 300\text{ cm}^{-1}$). This value is in good agreement with estimates for the S_1 energy of the carotenoids in LHC II.^{32,33} Since several different carotenoids can contribute to the observed TPE spectrum and apparently a background of either Car S_2 states or Chl *b* states is present at the blue edge of the spectrum, we have not attempted to fit the spectrum to several Gaussian vibronic lines to determine the 0–0 transition. Therefore, the range for the 0–0 transition of the energy-transferring carotenoids has been estimated by using the onset ($\sim 650\text{--}670$ nm) of the spectrum in the red edge. The TPE spectrum peaks at about 2×600 nm and has a local minimum at 2×560 nm before it shows increasing absorptivity toward higher energies. The energetic difference between the shoulder in the red (~ 2

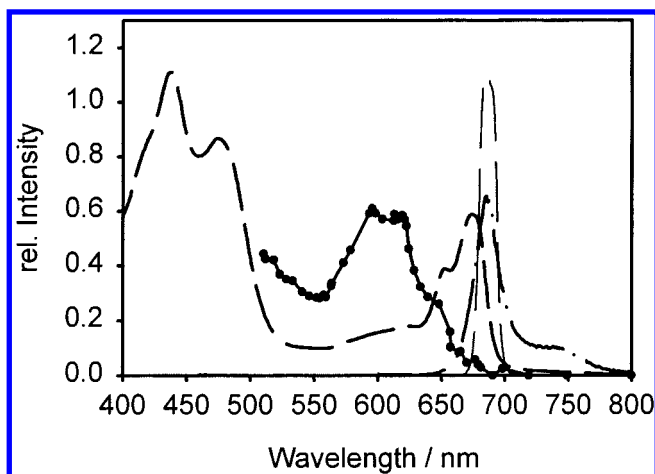


Figure 3. One-photon and two-photon spectra of LHC II. Two-photon excitation spectrum (solid line with circles). Absorption (long dashed line). Fluorescence (dash dotted line). Relative transmission of the interference filter used for the two-photon excitation experiment (thin dashed line).

$\times 650$ nm) and the maximum corresponds to ~ 1200 cm^{-1} , which is a reasonable value for C=C stretch vibrations of carotenoids. The bandwidth of the whole spectrum ($\sim 2 \times 650$ to 2×560 nm) is approximately 2500 cm^{-1} , which is in good agreement with known spectra of Car S_1 states.^{18,28,34–37}

We have to consider the possibility that one-photon allowed Chl-states contribute to the TPE spectrum. Shreve and co-workers measured the TPE spectrum of Chl in solution,³⁸ and observed no new bands that are not seen in one-photon spectroscopy. There are only minor differences in the relative intensities of the bands, but the Q_x band is still much smaller than the Q_y band. Our observed TPE band has a spectral position similar to that of the Chl Q_x band. However, in our TPE spectrum the Q_y band of Chl *a* is barely visible, and therefore contributions of one-photon-allowed Chl states in the Q_x region can be neglected. In the complex it is possible that excitonic interactions in Chl's may lead to new states that are two-photon-allowed.³⁹ Recently, states have been observed in IR absorption experiments of LH2 and reaction centers by Hochstrasser and co-workers, which do not correspond to known monomeric Chl states.^{40,41} However, since the excitonic interaction in LHC II should be much smaller (< 100 cm^{-1}) than in LH2, a significant contribution from such states seems unlikely.⁴²

Figure 4 shows the upconversion data and fits for the Chl Q_y emission. We excited at three different two-photon wavelengths (2×580 , 2×600 , and 2×610 nm). Since the traces showed no significant differences, they were added to improve the signal-to-noise ratio. Therefore, the shown data are the sum of the three traces and should be regarded as the Chl emission observed after broad band excitation between 2×580 and 2×610 nm. Repeating the measurements under identical conditions, but with only buffer as the sample, showed nothing but flat background. We deconvoluted the data with a triexponential function and found a 250 ± 50 fs rise and two decay times of 3 ps ($\sim 15\%$) and > 100 ps ($\sim 85\%$). No slow rise (> 1 ps) component was found. A double-exponential fit to the rise gives the two time constants of $\sim 200 \pm 100$ fs ($\sim 65 \pm 20\%$) and $\sim 600 \pm 200$ fs ($\sim 35 \pm 20\%$), but at the present signal-to-noise ratio too much significance should not be attached to these values. However, in recently measured pump-probe data, Gradinaru and co-workers reported some Car's with an S_1 lifetime of ~ 600 fs.²³ In our group similar results were found.²⁴ Although the first 1–2 ps can be affected by spectral evolution,

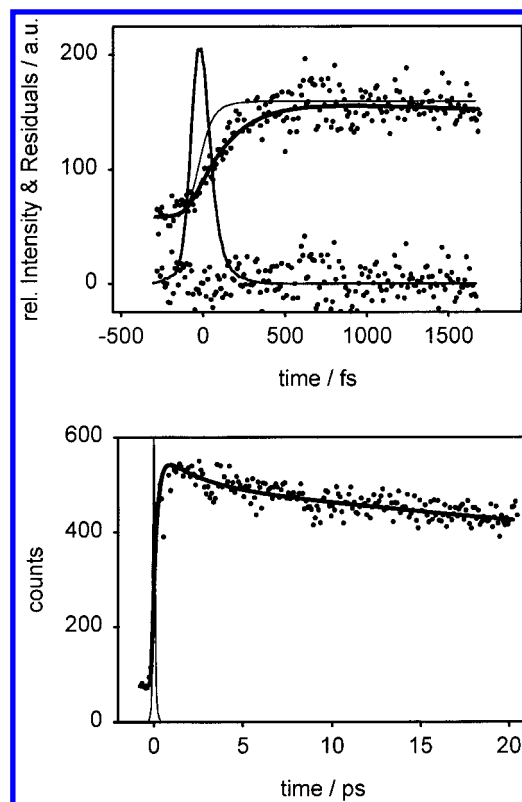


Figure 4. Top and bottom: Upconversion data after two-photon excitation at 2×580 to 2×610 nm and detection at 685 nm (circles), along with the exponential fit (thick lines). $\tau_1 = 250$ fs ($\sim 100\%$), $\tau_2 = 3$ ps (15%), $\tau_3 = 100$ ps (85%), residuals (circles), instrument response function (medium lines), and calculated curve corresponding to instantaneous rise (thin line).

IC of Chl's or ET between Chl's, the ET time constant, τ_{ET1} , cannot be much slower than the observed rise, because the ET is the limiting factor for the observation of any Chl fluorescence. Note that a contribution of Car S_1 fluorescence is extremely unlikely, since the corresponding transition is dipole-forbidden. Note also that a contribution of S_1 to ground-state IC to the observed rise can be neglected, since this IC is much slower. The small contribution of a 3 ps decay component is in good agreement with a dominant picosecond time constant reported by Peterman et al. (2.1 ps) and Holzwarth et al. (2.5 ps). From these transient absorption measurements this time constant appears to be connected with Chl *b* to Chl *a* transfer or to equilibration between Chl *a* pigments. However, in our case it also could reflect other processes such as vibrational cooling or excitation annihilation.

Figure 5 shows the upconverted Car S_2 ($\lambda_{\text{det}} = 575$ nm), Chl *a* ($\lambda_{\text{det}} = 685$ nm), and Chl *b* ($\lambda_{\text{det}} = 655$ nm) fluorescence after one-photon excitation at 500 or 510 nm (70–85% Car S_2 and 15–30% Chl *b* Soret). The Car S_2 fluorescence decays with the two time constants $\tau_{S_2} = 120 \pm 30$ fs (99%) and $\tau > 4$ ps (1%). The short time constant corresponds to the sum of the rates of internal conversion and energy transfer from S_2 , $\tau_{S_2}^{-1} = \tau_{IC}^{-1} + \tau_{ET2}^{-1}$. Very similar time constants were recently observed in pump-probe experiments as the rise of the Car $S_1 \rightarrow S_n$ excited state absorption: our group found for τ_{S_2} a value of $\sim 90 \pm 20$ fs at room temperature, and Gradinaru et al. found a value of ~ 100 fs at 77 K.^{23,24}

In a global analysis of all four Chl fluorescence traces ($\lambda_{\text{det}} = 655$ and 685 nm/ $\lambda_{\text{exc}} = 500$ and 510 nm) we fitted biexponential functions with a constant offset and found time constants of ~ 250 fs and ~ 2.3 ps. The Chl *b* fluorescence

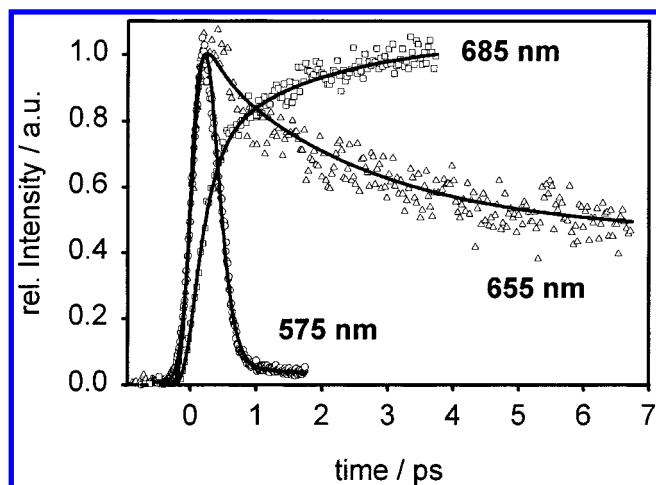


Figure 5. Upconversion data after one-photon excitation at 500 nm and detection at 575 nm (circles), 655 nm (triangles), and 685 nm (squares). (Data for excitation at 510 nm are similar.) Exponential fits (solid lines): (575 nm) 120 fs (99%) and 4.5 ps (1%); (655 nm) 250 fs (20%), 2.3 ps (40%), and 40% constant offset; (685 nm) 250 fs (−70%) and 2.3 ps (−30%).

decays with these two time constants (250 fs, +20%; 2.3 ps, +40%) to a constant value of ca. 40% of the initial fluorescence, whereas the Chl *a* fluorescence increases with the same constants (250 fs, −70%; 2.3 ps, −30%). Both constants are known to be connected to the Chl *b* to Chl *a* ET and intraband dynamics (i.e., Chl *a* → Chl *a* ET).²⁶ They also can be seen as a rise of the Chl *a* fluorescence (685 nm) after exciting Chl *b* at 655 nm (data not shown).⁴³ The larger relative amplitude of the 250 fs component in the Chl *a* trace is easily explained by an additional contribution of the fast Car → Chl *a* ET. It is not surprising that the rise in the Chl fluorescence (~250 fs) is much slower than the decay in the Car *S*₂ fluorescence (~120 fs), since in contrast to transient absorption experiments the Chl rise is convoluted by spectral cooling and internal conversion in the Chl's. In a similar study with *Rhodospseudomonas acidophila* the two corresponding time constants differed by 40–100 fs, depending on the detection wavelength in the BChl emission band.¹⁷ Furthermore, the rise in the Chl fluorescence is also convoluted by the slower ET from the Car *S*₁.

The difference in the relative amplitudes of the fast (250 fs) and slow (2.3 ps) components in the Chl *b* and Chl *a* fluorescence, respectively, suggests a large contribution of Car to Chl *a* ET. This is also supported by the fact that the Chl *b* fluorescence (655 nm) seems to have a much lower amplitude. On the other hand, comparison of amplitudes at different detection wavelengths in upconversion experiments is not very reliable, since they are very sensitive to the corresponding crystal angles.

Discussion

Time constants τ_{ET1} and τ_{ET2} . The most surprising result of our study is the very fast energy transfer from the dipole-forbidden Car *S*₁ state to the Chl's. To explore this issue, we first estimate the order of magnitude for the time constant τ_{ET1} for LHC II using known values of τ_{ET1} from other light-harvesting complexes and our observed TPE spectrum. A few examples of known Car *S*₁ to Chl ET (τ_{ET1}) time constants are peridinin to Chl *a* ET in the peridinin–Chl *a*–protein (PCP) from *Amphidinium carterae* (3.1 and 2.5 ps),^{18,44,45} spheroidene to BChl ET in *Rhodobacter sphaeroides* (2.0 ps),¹⁹ and okenone to BChl *a* ET in *Chromatium purpuratum* (3.8 and 0.5 ps).²⁰

The usual Fermi Golden Rule expression for the rate of energy transfer in the weak coupling limit is

$$k_{ET} = \frac{2\pi}{\hbar} |V|^2 J_{DA} \quad (1)$$

where V is the electronic coupling for a given mechanism and J_{DA} represents the density of energy-conserving states, i.e., the spectral overlap.¹⁵ It is still a matter of debate which mechanism applies for the Car *S*₁ to Chl ET. It was often assumed that a Dexter-type mechanism²¹ dominates the transfer; however, this assumption is unlikely to be correct.⁴⁶ The dependence of the electronic coupling $|V|^2$ on the donor–acceptor distance, r , of this mechanism can be approximated to be proportional to $|e^{-\beta/r}|^2 = e^{-2\beta/r}$, with β as the characteristic length, since it requires orbital overlap. However, in terms of the exchange mechanism the ET from the two-photon-allowed Car *S*₁ state to Chl has been shown to require *two* exchange interactions, and therefore the rate would be proportional to $e^{-4\beta/r}$, with β and r being on the same order of magnitude.⁴⁷ This results in much faster attenuation with r compared to other possible mechanisms such as quadrupole interactions or two-photon transitions, which do not depend on orbital overlap.⁴⁸ As a result of the uncertainty in the coupling mechanism we do not attempt to calculate the rate directly, but rather make an estimate of the rate by taking data from a protein complex in which we expect the electronic couplings to be most similar to those in LHC II. PCP should fulfill this requirement for the following reasons. The donor and acceptor pigments in both complexes are quite similar; furthermore, they all have similar separations, namely, van der Waals distance. In LHC II as well as in PCP there is a large orientational disorder of interacting donors and acceptors. Therefore, the orientational dependence of the electronic coupling should be roughly averaged out in both cases. Even though LHC II has a large excess of acceptors while PCP has a large excess of donors, the averaging of the couplings still should be similar, though this change in acceptor/donor ratio will clearly increase the Car to Chl energy transfer rate in LHC II. For an order of magnitude estimate of τ_{ET1} in LHC II using data from PCP we assume that it is sufficient to consider only the spectral overlap integral, J_{DA} , and the number of energy-accepting Chl's per Car, n_{Chl}/n_{Car} : $\tau_{ET1} \propto (J_{DA} n_{Chl}/n_{Car})^{-1}$.

We calculated for PCP and LHC II a relative spectral overlap integral, J_{rel} , by using the normalized measured or estimated Car *S*₁ emission spectra, $f_{Car}(\nu)$, the normalized absorption spectra of the acceptor, $\epsilon_{Chl}(\nu)$, and the stoichiometric ratio of Chl's to Car's in van der Waals contact, n_{Chl}/n_{Car} .¹⁵

$$J_{rel} = \frac{n_{Chl}}{n_{Car}} \times \frac{\int f_{Car}(\nu) \epsilon_{Chl}(\nu) d\nu}{\int f_{Car}(\nu) d\nu \int \epsilon_{Chl}(\nu) d\nu} \quad (2)$$

For the *S*₁ fluorescence, $f_{Car}(\nu)$, of LHC II we used the mirror image of the observed TPE spectrum, assuming a 0–0 transition of ~15 300 cm^{−1}. The *S*₁ fluorescence of peridinin in PCP is known. For the number of the accepting Chl's we only allowed Chl's to be included in the calculation, which the structure shows are likely energy acceptors from the Car's. In the case of LHC II we only included the seven most likely Chl *a*'s in van der Waals contact with the central two carotenoids ($n_{Chl}/n_{Car} = 3.5$). Consequently, we used for $\epsilon_{Chl}(\nu)$ only the absorption of the Chl *a* bands of LHC II. For *A. carterae* we allowed ET only to one Chl per Car ($n_{Chl}/n_{Car} = 1$). For the ratio $J_{rel}^{PCP}/J_{rel}^{LHC II}$ we obtained 0.12–0.15, depending on which of the reported τ_{ET1}^{PCP}

we used. The rate constant for LHC II can then roughly be estimated to be

$$\tau_{\text{ET1}}^{\text{LHC II}} \approx \frac{j_{\text{rel}}^{\text{PCP}}}{j_{\text{LHC II}}^{\text{PCP}}} \tau_{\text{ET1}}^{\text{PCP}} \approx 370\text{--}460 \text{ fs} \quad (3)$$

This very simple calculation shows that even with moderate pairwise Car S_1 to Chl ET rates, the large number of acceptors (Chl) in LHC II can easily explain a fast (sub picosecond) observed Car S_1 to Chl ET.

The same argument can be used for the energy transfer occurring from the Car S_2 state (P_2). For PCP Bautista et al.¹⁸ were able to conclude that almost all of the $\sim 90\%$ efficient Car \rightarrow Chl ET occurs via P_1 , i.e., via the S_1 state. Assuming a value of ~ 200 fs for $\tau_{\text{IC}}^{\text{PCP}}$ of peridinin and an efficiency for P_2 of not more than $\phi_{P_2}^{\text{PCP}} < 25\%$ in this protein complex, a value of at least $\tau_{\text{ET2}}^{\text{PCP}} = (1 - \phi_{P_2}^{\text{PCP}})/\phi_{P_2}^{\text{PCP}} \tau_{\text{IC}}^{\text{PCP}} > 600$ fs can be estimated. Since the normalized spectral overlaps of the Car S_2 emission and the Chl absorption for LHC II and PCP are very similar, the time constant for the P_2 ET in LHC II can immediately be estimated to be on the order of $\tau_{\text{ET2}}^{\text{LHC II}} \approx \tau_{\text{ET2}}^{\text{PCP}} (\phi_{\text{Chl}}^{\text{PCP}}/\phi_{\text{Car}}^{\text{PCP}}) / (\phi_{\text{Chl}}^{\text{LHC II}}/\phi_{\text{Car}}^{\text{LHC II}}) > 170$ fs. The P_2 ET is dominated by the Coulombic coupling mechanism, and therefore the electronic coupling could also be calculated more accurately by transition densities determined by quantum chemical methods.¹⁶ However, this will be the subject of future studies.

A more direct way to calculate $\tau_{\text{ET2}}^{\text{LHC II}}$ is by using the experimentally observed S_2 lifetime, τ_{S_2} , and the equation $\tau_{\text{ET2}}^{\text{LHC II}} = (\tau_{S_2}^{-1} - \tau_{\text{IC}}^{-1})^{-1}$. For τ_{S_2} we used the mean value $\tau_{S_2} \approx 105 \pm 25$ fs calculated from the time constants observed in this work ($\tau_{S_2} \approx 120 \pm 30$ fs) and in pump-probe data ($\tau_{S_2} \approx 90 \pm 20$ ^{23,24}). Assuming for τ_{IC} in LHC II a value of 215 ± 15 fs as measured for lutein¹² in solution, $\tau_{\text{ET2}}^{\text{LHC II}}$ becomes $\sim 230 \pm 100$ fs. This value is in very good agreement with the value estimated using the PCP data. As mentioned above, the much more rapid ET ($\tau_{\text{ET2}} \approx 50$ fs) observed in bacterial systems¹⁷ has its origin in the much larger splitting of Q_x and Q_y states of the BChl's compared to Chl. This results in a BChl Q_x state at higher energy, which has excellent spectral overlap with the Car S_2 state.

Which Chl's Accept the Energy from S_1 ? Our calculation of τ_{ET1} also suggests that it is likely that for pathway P_1 the energy is transferred predominantly to Chl a , because the spectral overlap of the Car S_1 emission is about 8 times larger with the absorption of Chl a than with that of Chl b . Furthermore, the lack of a slow rise component in the upconverted fluorescence upon TPE of the Car S_1 also indicates that the main part of the Car excitation energy is primarily transferred to Chl a . ET first to Chl b should appear in the data as a significant ($> 15\%$) picosecond Chl b to Chl a ET component with a negative amplitude.

Which Car's Are Energy Donors from S_1 ? The fast ET obtained after excitation into S_1 suggests that the major

contribution to our signals comes from the central Car's in LHC II, because they are in close proximity to a large number of energy-accepting Chl's. From the poorly resolved shape of our TPE it is not possible to judge whether only luteins or other carotenoids are energy donors. However, to explain the fast ET we observed, the 0-0 transition has to be around $15\,300 \text{ cm}^{-1}$ (650 nm) to allow a very good spectral overlap of the mirror image of the observed TPE spectrum with the Chl a absorption. Therefore, either the luteins (10 conjugated double bonds) have a relatively high S_1 energy or we primarily observed some Car's, such as violaxanthin or neoxanthin (9 conjugated double bonds). It is possible, that the luteins have a 0-0 transition corresponding to the small shoulder at around $14\,800 \text{ cm}^{-1}$ (670 nm) and have only a slower contribution to the kinetics, which is poorly resolved in our upconversion data. This could explain an additional time constant of ~ 600 fs which has been found recently for some carotenoids in LHC II in pump-probe experiments,^{23,24} because the spectral overlap is much smaller for Car's with a 0-0 transition at $14\,800 \text{ cm}^{-1}$. In that scenario, the spectral position of the larger shoulder is close to that expected for the 0-0 transition of violaxanthin or neoxanthin. Furthermore, this would confirm the results of Bassi and co-workers that at least some of these molecules must be in the central positions of the LHC II structure.⁷ On the other hand, a relatively high 0-0 transition of $15\,300 \text{ cm}^{-1}$ for lutein is also possible. In that case, the carotenoid in the protein environment must be optimized to shift the S_1 energy to a value for maximum ET to the Chl's.

What Are the Contributions of P_1 and P_2 to the Overall Car to Chl ET? With the information given above we are now able to make an estimate of the contributions of the P_1 and P_2 pathways to the overall Car \rightarrow Chl ET in LHC II. The efficiency of P_2 can be calculated as $\Phi_{P_2} = (\tau_{\text{ET2}}^{-1}/(\tau_{\text{ET2}}^{-1} + \tau_{\text{IC}}^{-1})) = 50 \pm 10\%$. The efficiency of P_1 then becomes $\Phi_{P_1} = \Phi_{\text{OA}} - \Phi_{P_2} = 30 \pm 10\%$, where $\Phi_{\text{OA}} \approx 80\%$ ¹² is the overall efficiency of Car \rightarrow Chl ET in LHC II. Note that we assumed that the difference of Φ_{OA} from 100% is entirely due to losses from the Car S_1 state. This is reasonable, because there is no major pathway for losing excitation energy after ET from the Car S_2 . Since a very fast (sub picosecond) ET is observed from the Car S_1 states, we must conclude that there are some Car's which transfer their energy very efficiently via S_1 , whereas others do not transfer at all and do not contribute to our TPE data. It seems likely that these Car's are the ones, with either a pure Chl b environment, with a 0-0 transition below the lowest Chl a states or which are located on the periphery of LHC II.

In Table 1 we have summarized some of the measured and calculated time constants and quantum yields relevant for the carotenoid to chlorophyll ET in LHC II. In this work we obtained for τ_{S_2} and τ_{ET1} values of 120 ± 30 and 250 ± 50 fs, whereas in pump-probe experiments 90 ± 20 fs^{23,24} and 600 ± 200 fs^{23,24} were obtained, respectively. For our calculations we used a mean value for τ_{S_2} of $\sim 105 \pm 25$. For τ_{IC} we used 215 ± 15 fs reported by Gillbro¹² for lutein. $\tau_{\text{OA}}^{\text{PP}}$ and $\tau_{\text{OA}}^{\text{UPC}}$ are

TABLE 1: Measured and Calculated Time Constants and Quantum Yields Relevant for the Carotenoid to Chlorophyll ET in LHC II^a

τ_{S_2}/fs	$\tau_{\text{ET2}}/\text{fs}$	$\tau_{\text{IC}}/\text{fs}$	$\tau_{\text{ET1}}/\text{fs}$	$\phi_{P_2}/\%$	$\phi_{P_1}/\%$	$\tau_{\text{OA}}^{\text{PP}}/\text{fs}$ ($\tau_{\text{rel}} = 0$ fs)	$\tau_{\text{OA}}^{\text{UPC}}/\text{fs}$ ($\tau_{\text{rel}} = 70$ fs)
$105 \pm 25^{23,24 b}$	230 ± 100^c	215 ± 15^{12}	250 ± 50^b	50 ± 10^c	30 ± 10^c	$230 \pm 50^{13 c}$	$270 \pm 50^{b,c}$
$105 \pm 25^{23,24 b}$	230 ± 100^c	215 ± 15^{12}	$600 \pm 200^{23,24}$	50 ± 10^c	30 ± 10^c	300 ± 80^c	370 ± 70^c

^a The time constants are defined in Figure 1. The quantum yields ϕ_{P_2} and ϕ_{P_1} refer to the percentage of the excitation energy initially located in the Car S_2 state, which is transferred to the chlorophylls via paths P_2 and P_1 , respectively. Data taken from the literature are indicated with numbers.

^b These values were measured in this work. ^c These values were calculated using the measured values in the same row.

the characteristic time constants for the overall Car \rightarrow Chl ET usually obtained as the rise in the Chl population in pump–probe experiments¹³ and upconversion experiments, respectively. In pump–probe experiments the measured rise in the Chl population is not convoluted by τ_{rel} , and therefore $\tau_{\text{OA}}^{\text{PP}}$ is generally smaller than $\tau_{\text{OA}}^{\text{UPC}}$. The measured values are $\tau_{\text{OA}}^{\text{PP}} = 220 \pm 25$ fs¹³ and $\tau_{\text{OA}}^{\text{UPC}} = 250$ fs. (The table only shows calculated values for $\tau_{\text{OA}}^{\text{PP}}$ and $\tau_{\text{OA}}^{\text{UPC}}$.) In the two different rows we used the two different values obtained for τ_{ET1} and the mean values for τ_{IC} and τ_{S_2} to calculate the other parameters. The time constants $\tau_{\text{OA}}^{\text{PP}}$ and $\tau_{\text{OA}}^{\text{UPC}}$ were obtained by fitting a monoexponential rise to Chl population curves calculated using the kinetic model described in ref 17. Note that describing the rise in the Chl population monoexponentially is only an approximation, which is usually done in the analysis of the pump–probe and upconversion data, because the several very similar time constants contributing to the kinetics of this rise cannot be resolved properly. For calculating $\tau_{\text{OA}}^{\text{PP}}$ we used $\tau_{\text{rel}} = 0$ fs, whereas for calculating $\tau_{\text{OA}}^{\text{PP}}$ and $\tau_{\text{OA}}^{\text{UPC}}$ we used $\tau_{\text{rel}} = 70$ fs.

Table 1 shows that better agreement with the measured values for $\tau_{\text{OA}}^{\text{PP}}$ (220 ± 25 fs)¹³ and $\tau_{\text{OA}}^{\text{UPC}}$ (250 fs) is found by using 250 ± 50 fs for τ_{S_1} . However, using $\tau_{\text{S}_1} = 600 \pm 200$ fs also yielded reasonable agreement between the measured and calculated $\tau_{\text{OA}}^{\text{PP}}$ and $\tau_{\text{OA}}^{\text{UPC}}$.

Conclusion

By measuring the two-photon excitation spectrum of LHC II, we have shown that the lowest excited states of the Car's, which are able to transfer energy to the Chl's, have a 0–0 transition around $15\,100 \pm 300$ cm⁻¹. The time dependence of the Chl fluorescence after two-photon excitation shows that there is a very fast ($\sim 250 \pm 50$ fs) ET from the one-photon-forbidden Car S₁ to the Chl's. From a simple calculation of this time constant in LHC II ($\sim 400 \pm 200$ fs) we conclude that this transfer is on the sub picosecond time scale because the Car's in LHC II are surrounded by a large excess of energy-accepting Chl's. The time dependence of the upconverted Car S₂ fluorescence shows that the lifetime of the Car S₂ state is about 120 ± 30 fs. The time dependence of the upconverted Chl *a* (685 nm) and Chl *b* (655 nm) fluorescence after excitation into the dipole-allowed Car S₂ state (500–510 nm) is in good agreement with earlier data from similar pump–probe experiments.^{12,13} Together with the TPE experiments these results suggest that the excitation energy from the Car S₁ state is predominantly transferred to Chl *a*. With the observed results we are able to give an estimate for the quantum yield of the Car to Chl ET via the Car S₂ state of $\sim 50 \pm 10\%$. For the quantum yield of the Car to Chl ET via the Car S₁ state we estimated a value of $\sim 30 \pm 10\%$.

Acknowledgment. We thank Profs. A. P. Shreve and A. C. Albrecht for sharing with us the results of their two-photon experiments of Chl *a*. We thank Prof. J. Wright and Dr. G. D. Scholes for helpful suggestions. We also thank F. Calkoen, H. van Amerongen, and co-workers for generously providing us with some of their LHC II preparations. This work was supported by the Director, Office of Science, Office of Basic Energy Sciences, Chemical Sciences Division of the U.S. Department of Energy under Contract No. DE-AC03-76SF00098. P.J.W. is grateful for financial support from the Deutsche Forschungsgemeinschaft.

References and Notes

- (1) van Grondelle, R.; Dekker, J. P.; Gillbro, T.; Sundström, V. *Biochim. Biophys. Acta* **1994**, *1187*, 1–65.
- (2) Jansson, S. *Biochim. Biophys. Acta* **1994**, *1184*, 1–19.
- (3) Jennings, R. C.; Bassi, R.; Zucchelli, G. *Top. Curr. Chem.* **1996**, *177*, 147–181.
- (4) Siefermann-Harms, D. *Biochim. Biophys. Acta* **1985**, *811*, 325–355.
- (5) Peterman, E. J. G.; Calkoen, F.; Gradinaru, C.; Dukker, F. M.; van Grondelle, R.; van Amerongen, H. *Photosynthesis: from light to biosphere*; Kluwer Academic Publishers: Dordrecht, The Netherlands, 1995; Vol. IV, pp 31–34.
- (6) Kühlbrandt, W.; Wang, D. N.; Fujiyoshi, Y. *Nature* **1994**, *367*, 614–621.
- (7) Croce, R.; Weiss, S.; Bassi, R. *J. Biol. Chem.* **1999**, *274*, 29613–29623.
- (8) Frank, H. A.; Cogdell, R. J. *Photochem. Photobiol.* **1996**, *63*, 257–264.
- (9) Ruban, A. V.; Young, A. J.; Horton, P. *Biochemistry* **1996**, *35*, 674–678.
- (10) Horton, P.; Ruban, A. V.; Walters, R. G. *Annu. Rev. Plant* **1996**, *47*, 655–684.
- (11) Bergantino, E.; Dainese, P.; Cerovic, Z.; Sechi, S.; Bassi, R. *J. Biol. Chem.* **1995**, *270*, 8474–8481.
- (12) Connelly, J. P.; Müller, M. G.; Bassi, R.; Croce, R.; Holzwarth, A. R. *Biochemistry* **1997**, *36*, 281–288.
- (13) Peterman, E. J. G.; Monshouwer, R.; van Stokkum, I. H. M.; van Grondelle, R.; van Amerongen, H. *Chem. Phys. Lett.* **1997**, *264*, 279–284.
- (14) Macpherson, A. N.; Gillbro, T. *J. Phys. Chem. A* **1998**, *102*, 5049–5058.
- (15) Förster, T. (a) *Ann. Phys.* **1948**, *2*, 55–75. (b) *Fluoreszenz organischer Verbindungen*; Vandenhoeck and Ruprecht: Göttingen, 1951.
- (16) Krueger, B. P.; Scholes, G. D.; Fleming, G. R. *J. Phys. Chem B* **1998**, *102*, 5378–5386.
- (17) Krueger, B. P.; Scholes, G. D.; Jimenez, R.; Fleming, G. R. *J. Phys. Chem. B* **1998**, *102*, 2284–2292.
- (18) Bautista, J. A.; Hiller, R. H.; Sharples, F. P.; Gosztola, D.; Wasielewski, M.; Frank, H. A. *J. Phys. Chem A* **1999**, *103*, 2267–2273.
- (19) Zhang, J. P.; Koyama, Y. Unpublished results.
- (20) Andersson, P. O.; Cogdell, R. J.; Gillbro, T. *Chem. Phys.* **1996**, *210*, 195–217.
- (21) Dexter, D. L. *J. Chem. Phys.* **1953**, *21*, 836–850.
- (22) Friedrich, M. *J. Chem. Educ.* **1982**, *59* (6), 472–481.
- (23) Gradinaru, C. C.; van Stokkum, I. H. M.; van Grondelle, R.; van Amerongen, H. Results presented at the Workshop “Interactions between Chlorophylls and Carotenoids in Photosynthesis” in Antalya, Turkey, 1999.
- (24) Walla, P. J.; Yom, J.; Fleming, G. R. Unpublished results.
- (25) Croce, R.; Müller, M. G.; Bassi, R.; Holzwarth, A. R. Results presented at the Workshop “Interactions between Chlorophylls and Carotenoids in Photosynthesis” in Antalya, Turkey, 1999.
- (26) Agarwal, R.; Krueger, B. P.; Scholes, G. D.; Yang, M.; Yom, J. M.; Fleming, G. R. *J. Phys. Chem. B* **2000**, *104*, 2908–2918.
- (27) Peterman, E. J. G.; Dukker, F. M.; van Grondelle, R.; van Amerongen, H. *Biophys. J.* **1995**, *69*, 2670–2678.
- (28) Krueger, B. P.; Yom, J.; Walla, P. J.; Fleming, G. R.; *Chem. Phys. Lett.* **1999**, *310*, 57–64.
- (29) Birge, R. R. In *Ultrasensitive Laser Spectroscopy*; Kliger, Ed.; Academic Press: New York, 1983; pp 109–174.
- (30) Walker, G. C.; Jarzeba, W.; Kang, T. J.; Johnson, A. E.; Barbara, P. F. *J. Opt. Soc. Am. B* **1990**, *7*, 1521–1527.
- (31) Mokhtari, A.; Chebira, A.; Chesnoy, J. J. *Opt. Soc. Am. B* **1990**, *7*, 1551–1557.
- (32) Chynvat, V.; Frank, H. A. *Chem. Phys.* **1995**, *194*, 237–244.
- (33) Polivka, T.; Herek, J. L.; Zigmantas, D.; Åkerlund, H. E.; Sundström, V. *Proc. Natl. Acad. Sci. U.S.A.* **1999**, *96*, 4914–4917.
- (34) Fujii, R.; Onaka, K.; Kuki, M.; Koyama, Y.; Watanabe, Y. *Chem. Phys. Lett.* **1998**, *288*, 847–853.
- (35) Sashima, T.; Shiba, M.; Hashimoto, H.; Nagae, H.; Koyama, Y. *Chem. Phys. Lett.* **1998**, *290*, 36–42.
- (36) Shreve, A. P.; Trautmann, J. K.; Owen, T. G.; Albrecht, A. C. *Chem. Phys. Lett.* **1990**, *170*, 51–56.
- (37) Desamero, R. Z. B.; Chynwat, V.; van der Hoef, I.; Jansen, F. J.; Lugtenburg, J.; Gosztola, D.; Wasielewski, M. R.; Cua, A.; Bocian, D. F.; Frank, H. A. *J. Phys. Chem. B* **1998**, *102*, 8151–8162.
- (38) Shreve, A. P. Private communication.
- (39) Scherer, P. O. J.; Fischer, S. F. *Chem. Phys. Lett.* **1997**, *268*, 133–142.
- (40) R. M. Hochstrasser and co-workers. Unpublished results.

- (41) Wynne, K.; Haran, G.; Reid, G. D.; Moser, C. C.; Dutton, P. L.; Hochstrasser, R. M. *J. Phys. Chem.* **1996**, *100*, 5140–5148.
- (42) Trinkunas, G. Conelly, J. P.; Müller, M. G.; Valkunas, L.; Holzwarth, A. R. *J. Phys. Chem. B* **1997**, *101*, 7313–7320.
- (43) Du, M.; Xie, X.; Mets, L.; Fleming, G. R. *J. Phys. Chem.* **1994**, *98*, 4736–4741.
- (44) Lampoura, S. S.; B. P. Krueger, van Amerongen, H.; van Grondelle, R. results presented at the Workshop “Interactions between Chlorophylls and Carotenoids in Photosynthesis” in Antalya, Turkey, 1999.
- (45) Macpherson, A. N.; Hiller, R. G.; Hoffmann, E.; Gillbro, T. Results presented at the Workshop “Interactions between Chlorophylls and Carotenoids in Photosynthesis” in Antalya, Turkey, 1999.
- (46) Scholes, G. D.; Harcourt, R. D.; Fleming, G. R. *J. Phys. Chem. B* **1997**, *101* (37), 7302–7312.
- (47) Scholes, G. D. Private communication.
- (48) Allcock, P.; Andrews, D. L. *J. Chem. Phys.* **1998**, *108*, 3089–3095.